

THE NONLINEAR SOLAR DYNAMO AND DIFFERENTIAL ROTATION: A TAYLOR NUMBER PUZZLE ?

A. BRANDENBURG¹, D. MOSS^{1,2}, G. RÜDIGER³, and I. TUOMINEN¹

(Received 9 August, 1989; in revised form 29 September 1989)

Abstract. We consider dynamically consistent mean-field dynamos in a spherical shell of incompressible fluid. The generation of magnetic field and differential rotation is parameterized by the α - and Λ -effects, respectively. Extending previous investigations, we include now the cases of moderate and rapid rotation in the sense that the inverse Rossby number can approach or exceed unity. This can lead to *disk-shaped* Ω -contours, which are in better accordance with recent results of helioseismology than *cylindrical* Ω -contours. On the other hand, in order to obtain $\alpha\omega$ -dynamo cycles the Taylor number has to be so large, that eventually cylindrical Ω -contours become unavoidable (cf. Taylor–Proudman theorem). We discuss the different possibilities in a state diagram, where the inverse Rossby number and the relative correlation length are taken as the elementary parameters for mean-field dynamos.

1. Introduction

The nature of the solar dynamo has become a matter of debate since recent results of helioseismology provided new constraints for the internal angular velocity of the Sun (e.g., Brown and Morrow, 1987; Libbrecht, 1988; Dziembowski, Goode, and Libbrecht, 1989). Attempts have been made to develop models that account for these new constraints (cf. Gilman, Morrow, and DeLuca, 1989). In the present paper we discuss how far we can understand the solar dynamo in terms of the traditional $\alpha\omega$ -concept by including also the momentum equation for the mean motion.

Many features of the solar magnetic field can be reproduced already in the framework of kinematic (linear) dynamo models where the profiles for α - and ω -effect are prescribed according to results from the mixing-length approach and from helioseismology, respectively (cf. Brandenburg and Tuominen, 1988). However, the nonlinear nature of the solar dynamo is also quite apparent. The variation of sunspot number is aperiodic and the occurrence of grand minima is irregular. The number of sunspots in the northern and southern hemisphere is not the same and there is evidence for long-term variations of the symmetry properties of the solar mean magnetic field (Brandenburg *et al.*, 1989; Brandenburg, Krause, and Tuominen, 1989).

Also from a theoretical point of view one ‘needs’ nonlinear effects, because the dynamo equation (cf. Krause and Rädler, 1980)

$$\partial \langle \mathbf{B} \rangle / \partial t = \text{curl}(\langle \mathbf{u} \rangle \times \langle \mathbf{B} \rangle + \alpha \langle \mathbf{B} \rangle - \eta_t \text{curl} \langle \mathbf{B} \rangle), \quad (1)$$

with constant macro- and micro-velocity fields, is linear in $\langle \mathbf{B} \rangle$ and the solution is,

¹ Observatory and Astrophysics Laboratory, University of Helsinki, Tähtitorninmäki, SF-00130 Helsinki, Finland.

² Dept. of Mathematics, The University, Manchester M13 9PL, England.

³ Sternwarte Babelsberg, Academy of Science of GDR, 1591 Potsdam, G.D.R.

therefore, proportional to $e^{\lambda t}$ (λ is complex). The molecular magnetic diffusivity is neglected compared with the turbulent magnetic diffusivity, η_t . For sufficiently strong (supercritical) α the exponential growth of $\langle \mathbf{B} \rangle$ can only be halted by a nonlinear feedback, either on α or on the mean velocity $\langle \mathbf{u} \rangle$. In both cases the feedback comes via the Lorentz force terms in the momentum equation. In the following we shall distinguish between these feedbacks by referring to them as micro- and macro-feedback, respectively, because α is affected by the Lorentz force acting on the small-scale motions while $\langle \mathbf{u} \rangle$ represents the large scale motions.

The micro-feedback is quantitatively not very well understood and it would, therefore, be helpful if its importance relative to that of the macro-feedback was small. (This may or may not be true in practice!) This point will be examined in the first section. The role of the mean-field momentum equation is not only that it provides the macro-feedback, but also that it determines the differential rotation law. As a simplification the differential rotation has often been taken from the observations rather than being computed as a self-consistent solution of the momentum equation.

In the framework of mean-field theory the differential rotation can be generated by the non-diffusive parts of the Reynolds stress tensor components $\langle u'_r u'_\phi \rangle$ and $\langle u'_\theta u'_\phi \rangle$ which are parameterized by the Λ -effect, i.e., by Λ_V and Λ_H , respectively. (Primes refer to the fluctuating quantities.) We follow here the concept introduced by Rüdiger (1980, 1989). Dynamo models with constant Λ_V and vanishing Λ_H have been recently investigated by Brandenburg *et al.* (1990, hereafter Paper I) and the basic results will be discussed in Section 3. The assumption of neglecting $\langle u'_\theta u'_\phi \rangle$, and thereby also of Λ_H , is appropriate in the case of slow rotation, in the sense that $\text{Ro}^{-1} \equiv 2\Omega_0 \tau_{\text{cor}} \ll 1$. This is not justified for the Sun. We shall, therefore, extend our previous models to the case of moderate rotation, including the effect of Λ_H . Our conclusions will be given in the last section.

2. The Relative Importance of Micro- and Macro-Feedback

The quantities α and η_t in Equation (1) parameterize the correlation between the fluctuations \mathbf{u}' and \mathbf{B}' with

$$\langle \mathbf{u}' \times \mathbf{B}' \rangle = \alpha \langle \mathbf{B} \rangle - \eta_t \text{curl} \langle \mathbf{B} \rangle \quad (2)$$

(Krause and Rädler, 1980). We neglect here the possibility that α and η_t can be tensors. However, there can be a functional dependence of α (and η_t) on $\langle \mathbf{B} \rangle$ (Rüdiger, 1974; Roberts and Soward, 1975) which is complicated and unfortunately also still not well-determined for solar and stellar conditions. The approximate result for weak fields is

$$\alpha = \alpha_0 (1 - \langle \mathbf{B} \rangle^2 / B_0^2), \quad (3)$$

where $\alpha_0 \approx \Omega l \cos \theta$ is a correlation length. B_0^2 is related to the turbulent pressure

$$B_0^2 / \mu \approx \rho u_t^2 \quad (4)$$

(Kleeorin and Ruzmaikin, 1982). The r.m.s.-velocity of the turbulence, u_t , does not

directly enter into the mean-field equations, but only via the turbulent magnetic diffusivity

$$\eta_t = C_\eta u_t l, \quad (5)$$

where C_η is a factor typically between $\frac{1}{3}$ and $\frac{1}{10}$ (Parker, 1979). Inserting u_t from Equation (5) into Equation (4) we find

$$B_0^2 \approx \alpha_B^{-1} (\mu \rho \eta_t^2 / R^2), \quad (6)$$

where $\alpha_B = C_\eta^2 \xi^2$ and $\xi = l/R$ is the correlation length relative to the solar radius R .

From now on we shall use only dimensionless quantities, measuring length in units of R and time in units of the turbulent diffusion time R^2/η_t . Velocity (and α) is measured in units of η_t/R and \mathbf{B} in units of $\eta_t/R \sqrt{\mu\rho}$. Equation (3) becomes then

$$\alpha = C_\alpha \cos \theta (1 - \alpha_B \langle \mathbf{B} \rangle^2), \quad (7)$$

where we have introduced the abbreviation $C_\alpha = \frac{1}{2} P_m \text{Ta}^{1/2} \xi$. Here, $\text{Ta} = (2\Omega_0 R^2 / \nu_t)^2$ is the Taylor number and $P_m = \nu_t / \eta_t$ the turbulent magnetic Prandtl number (ν_t is kinematic turbulent viscosity). For simplicity we assume the quantities ν_t , η_t , u_t , and l to be constant. Physically we expect $\alpha \rightarrow 0$ as $\langle \mathbf{B} \rangle \rightarrow \infty$. As a numerically convenient extension of Equation (7) for arbitrary field strength we adopt in the following the form $\alpha = C_\alpha \cos \theta / (1 + \alpha_B \langle \mathbf{B} \rangle^2)$.

The total energy of the mean magnetic field, $E = \frac{1}{2} \int \langle \mathbf{B} \rangle^2 dV$, grows approximately linearly with C_α (see Figure 8(a) and Figure 9(a) in Brandenburg *et al.*, 1989). For the α^2 -dynamo we find the following scaling approximations:

$$E \approx 0.12 (C_\eta \xi)^{-2} (C_\alpha - C_\alpha^{(A)}) \quad (\text{micro-feedback}), \quad (8)$$

$$E \approx 54 (C_\alpha - C_\alpha^{(A)}) \quad (\text{macro-feedback}), \quad (9)$$

where $C_\alpha^{(A)}$ is the marginal dynamo number for the antisymmetric (A -type or dipole-type) solution. The importance of the micro- and macro-feedback terms is equal when $\xi = \xi_{\text{crit}} \approx 0.05/C_\eta = 0.15 \dots 0.5$, depending on the value chosen for C_η . Macro-feedback dominates over micro-feedback for small values of ξ . For oscillatory $\alpha\omega$ -dynamos the scaling approximations are:

$$E \approx 1.6 \times 10^{-4} (C_\eta \xi)^{-2} (C_\alpha - C_\alpha^{(A)}) C_\omega \quad (\text{micro-feedback}), \quad (10)$$

$$E \approx 0.37 (C_\alpha - C_\alpha^{(A)}) 0.7 V^{(0)} P_m \text{Ta}^{1/2} \quad (\text{macro-feedback}) \quad (11)$$

(see Figure 11 in Brandenburg, Krause, and Tuominen, 1989 and Table 8 in Brandenburg *et al.*, 1990). In the case of Equation (11) the differential rotation is generated by the A -effect, for which in a full sphere $C_\Omega \approx 0.7 V^{(0)} P_m \text{Ta}^{1/2}$. The micro- to macro-feedback terms are of comparable importance when $\xi = \xi_{\text{crit}} \approx 0.02/C_\eta = 0.06 \dots 0.2$, that is for a given value of ξ the $\alpha\omega$ -dynamo is more sensitive to micro-feedback than then α^2 -dynamo.

When l is identified with the mixing-length from standard solar envelope models we have at the bottom of the convection zone $\xi \approx 0.13$. Thus the importance of both

feedbacks is then roughly equal. In upper layers with $\xi < \xi_{\text{crit}}$ the macro-feedback may play a more important role. However, it is not justified to draw detailed conclusions for the Sun, because the models with macro-feedback are based on an incompressible fluid.

So far ξ is, in principle, a free parameter. As mentioned above, ξ might be chosen to be in agreement with the value for the solar convection zone at some level. No further constraints on ξ exists for these models. In the next section we shall see that the mechanism for the generation of differential rotation also involves ξ as a parameter, which leads then to a further constraint.

3. Dynamos with Differential Rotation

3.1. THE BASIC EQUATIONS

Here, as in Paper I, we consider the initial value problem of an incompressible, and conducting fluid with *constant* density, ρ , in a rotating shell with inner and outer radii R_0 and R , respectively. We solve the dynamo equation (1) together with the momentum equation in an inertial frame of reference, starting with a rigid rotation with angular velocity, Ω_0 , and a weak ‘seed’ magnetic field. The momentum equation for the mean fields is, in dimensionless form,

$$\frac{D\langle \mathbf{u} \rangle}{Dt} = -\nabla \mathcal{P} - \langle \mathbf{B} \rangle \times \text{curl} \langle \mathbf{B} \rangle - \text{div}(\mathcal{Q} - \mathcal{B}), \quad (12)$$

where \mathcal{P} is a reduced pressure (including gravitational potential and turbulent magnetic pressure). Similarly to the α -effect in the induction equation, the new terms $\mathcal{Q}_{ij} = \langle u'_i u'_j \rangle$ and $\mathcal{B}_{ij} = \langle B'_i B'_j \rangle$ now appear. As in Paper I we neglect \mathcal{B} and adopt for \mathcal{Q} the form

$$\mathcal{Q}_{ij} = A_{ijk} \Omega_k - N_{ijkl} \partial_l \langle u_k \rangle, \quad (13)$$

where $\Omega = \hat{\mathbf{z}} \langle u_\phi \rangle / r \sin \theta$ and $\hat{\mathbf{z}}$ is the unit vector along the axis of rotation. The second term on the right-hand side of Equation (13) describes a diffusive transport of angular momentum. The tensor N_{ijkl} is in general anisotropic. For simplicity we neglect here such effects and take $N_{ijkl} = P_m (\delta_{ik} \delta_{jl} + \delta_{jk} \delta_{il}) + \dots$ (here, the dots indicate the presence of a further term proportional to $\delta_{ij} \delta_{kl}$ which, however, gives no contribution for a solenoidal flow). In Equation (12) the molecular kinematic viscosity is neglected against ν_t . The A -term depends essentially on the anisotropic nature of the turbulence. Rüdiger (1980) employed an expansion for A which is, in dimensionless form,

$$\begin{aligned} A_V \Omega &\equiv (\Lambda \Omega)_{r\phi} / \sin \theta = P_m (V^{(0)} + V^{(1)} \sin^2 \theta + \dots) \Omega, \\ A_H \Omega &\equiv (\Lambda \Omega)_{\theta\phi} / \cos \theta = P_m (H^{(1)} \sin^2 \theta + \dots) \Omega. \end{aligned} \quad (14)$$

$V^{(0)}$ is of order of unity and $V^{(1)}$ and $H^{(1)}$ are expected to scale quadratically with the inverse Rossby number

$$\text{Ro}^{-1} \equiv 2\Omega_0 \tau_{\text{cor}} = P_m \text{Ta}^{1/2} C_\eta \xi^2. \quad (15)$$

Introducing a scaling factor ζ we write $V^{(1)} = H^{(1)} = \zeta^2 \text{Ro}^{-2}$. Using the definition of C_α we have $\text{Ro}^{-1} = 2C_\alpha \alpha_B^{1/2}$. From this expression we see that the micro-feedback and the higher-order terms in the \mathcal{A} -effect become simultaneously important (i.e., $\alpha_B = O(1)$ and $V^{(1)} = H^{(1)} = O(1)$) when $\zeta = \zeta_{\text{crit}} \equiv (2C_\alpha)^{-1}$. The results for C_α and $\zeta^2 \text{Ro}^{-2}$ for different values of Ta and ξ are given in Table I.

TABLE I

The scaling results for C_α and Ro^{-2} for different values of Ta and ξ for $C_\eta = 0.32$. The values for $C_\alpha = 5$ are marked in bold (see text).

$\alpha_B \rightarrow$ $P_m^2 \text{Ta} \downarrow$	10^{-1} $\xi = 1$	10^{-3} 0.01	10^{-5} 0.01	10^{-7} 0.001
10^2	5 10	0.5	10^{-3}	0.05 10^{-7}
10^4	50 10^3	5 10^{-1}	0.5	10^{-5}
10^6	500 10^5	50	10	5 10^{-3}
10^8	5000 10^7	500	10^3	50 10^{-1}

Our previous dynamo models of Paper I, where only macro-feedback is considered, have been computed for slightly supercritical values of C_α between 5 and 15 (depending on the Taylor number). Table I shows that the corresponding values of ξ vary between 1 (for $\text{Ta} = 10^2$) and 10^{-3} (for $\text{Ta} = 10^8$). The related values of $V^{(1)}$ and $H^{(1)}$ vary between 1 and 10^{-6} . In this sense higher order terms in the \mathcal{A} -effect seem to be negligible for $\text{Ta} \geq 10^6$. This is at first glance surprising, since one would expect that large Taylor numbers and large inverse Rossby numbers correspond to the same limit. (Note, however, that this is a consequence of treating only slightly supercritical values of C_α .)

3.2. DISK-SHAPED Ω -CONTOURS

In the case of large Taylor numbers the contours of constant angular velocity lie on cylinders. This is not in agreement with recent results of helioseismology (Libbrecht, 1988; Brown and Morrow, 1987) and such models fail, therefore, to explain the geometry of the solar angular velocity, which seems to be more ‘disk-shaped’ than cylindrical.

Disk-shaped angular velocity profiles result when higher-order terms in the \mathcal{A} -effect are taken into account (Rüdiger, 1989; Tuominen and Rüdiger, 1989). In Figure 1 (upper row) we show the Ω -contours for various Taylor numbers for the case $V^{(0)} = -1$ and $V^{(1)} = H^{(1)} = 1$ and with ξ being small enough so that no magnetic field is generated. For small values of Ta the angular velocity is clearly a function of $z \equiv r \cos \theta$. Note that the angular velocity is constant in the equatorial plane. Furthermore, it becomes evident that the disk-shaped Ω -contours change to cylindrical contours as Ta is increased. The transition from disk-shaped to cylindrical contours happens between $\text{Ta} = 10^4$ and $\text{Ta} = 10^6$. It seems, therefore, that, assuming our model with its many simplifications has some validity, then in the Sun the Taylor number cannot exceed a value of about 10^5 . This corresponds to a value of $v_t \approx 10^{14} \text{ cm}^2 \text{ s}^{-1}$, i.e., about one order of magnitude higher than the values usually adopted.

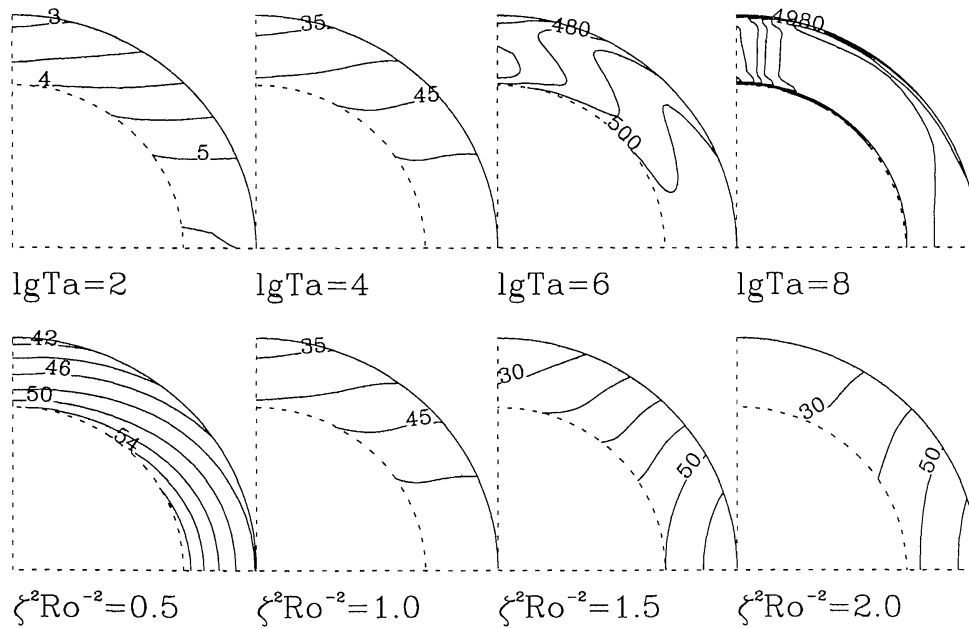


Fig. 1. Contours of constant Ω for different Taylor numbers (upper row, for $\zeta \text{Ro}^{-1} = 1$) and different values of ζRo^{-1} (lower row, for $\text{Ta} = 10^4$). $V^{(0)} = -1$.

Since disk-shaped contours are favoured as ζRo^{-1} increases one might guess that one might delay the onset of the Taylor–Proudman effect by increasing ζRo^{-1} sufficiently. This is, however, *not* the case. In Figure 1 (lower row) we have plotted Ω -contours for different values of ζRo^{-1} , keeping $\text{Ta} = 10^4$ and $V^{(0)} = -1$. For $0 < \zeta \text{Ro}^{-1} < 1$ we have the interesting case of equatorial acceleration together with $\partial\Omega/\partial r < 0$. For $\zeta \text{Ro}^{-1} \geq 1$ there is a certain latitude where $\partial\Omega/\partial r \approx 0$. (This position moves away from the equator as Ro^{-1} is increased.) This case was discussed already by Kichatinov (1987). For $\zeta^2 \text{Ro}^{-2} \gtrsim 2$ the Ω -contours tend to be cylindrical even for relatively small Taylor numbers. Thus, for the Sun we expect $\zeta \text{Ro}^{-1} \approx 1$, or slightly larger.

3.3. DYNAMOS WITH DISK-SHAPED Ω -CONTOURS

We investigate now the possibility of dynamo action for the case where the Ω -contours are disk-shaped and we take therefore $V^{(0)} = -1$ and $\zeta \text{Ro}^{-1} = 1$. The dynamo starts to operate for $\text{Ta} \geq 10^4$ when $\xi = 0.28$ and $C_\eta \zeta = 0.13$, where we have assumed $P_m = 1$. This corresponds to $C_\alpha = 14$. The resulting field and flow configuration is displayed in Figure 2. Note the concentration of magnetic energy close to the poles. The field is stationary, but becomes oscillatory for $C_\alpha \geq 20$, i.e., for $\xi > 0.4$ and $C_\eta \zeta < 0.06$. Snapshots for such a solution are given in the last three columns of Figure 2. The field geometry and the strong gradients of the angular velocity at the poles due to the magnetic feedback are unrealistic for solar application.

From previous investigations (Paper I) it is clear that magnetic cycles with field migration close to the equator are possible only if $P_m^2 \text{Ta} \gtrsim 10^{7 \dots 8}$. In order to keep still the disk-shaped Ω -contours we are forced to have $\text{Ta} \lesssim 10^{4 \dots 5}$, in other words

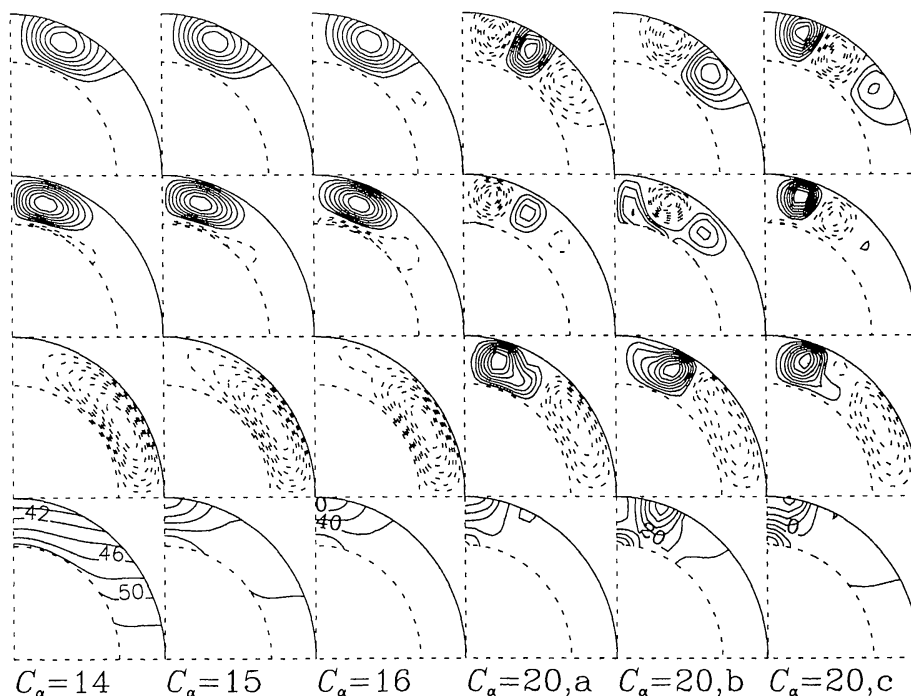


Fig. 2. The field geometry for models with different values of C_α with $V^{(0)} = -1$ and $\zeta \text{Ro}^{-1} = 1$. In the first row the magnetic field lines of the poloidal field are plotted, in the second row contours of constant toroidal field, in the third row stream lines of the meridional motion, and in the last row contours of constant angular velocity. Dashed contours refer to negative values (or poleward circulation in the third row). In the last three columns are snapshots (a, b, and c) for $C_\alpha = 20$. The time difference between each of them is 0.085.

$P_m \gtrsim 10 \dots 100$. It is not only theoretically rather hopeless to explain such an extreme value for the (turbulent) magnetic Prandtl number, but also does not even lead to the expected oscillatory dynamo solutions.

4. Discussion

The present investigations have shown that already simple incompressible dynamo models with dynamically constrained differential rotation and meridional circulation can illuminate some problems of the solar dynamo. The micro-feedback and higher order terms in the Λ -effects complicates the situation, because new unknown parameters are involved. Including various scaling dependencies of the different mean-field transport coefficients reduces the number of free parameters or at least puts limits to them. This becomes additionally important once even more ill-known parameters are included. For example, not only α but also η , and, in particular, also Λ can be quenched by the magnetic field (Kichatinov, 1988; Rüdiger and Kichatinov, 1990).

It seems that the solar disk-shaped Ω -contours provide an important constraint for hydromagnetic dynamo models. However, there is a dilemma: one wants the Ω -effect (differential rotation) to be strong enough to allow oscillatory dynamo solutions with field migration close to the equator. This requires also a rapid rotation, i.e., a high Taylor number. On the other hand one wants the Taylor number to be sufficiently small,

because otherwise disk-shaped Ω -contours become impossible. Thus, obviously, the solar dynamo operates in a regime of intermediate rotation rate.

It appears useful to take the relative correlation length, ξ , and the inverse Rossby number, Ro^{-1} , as the elementary parameters of the dynamo. Additionally, C_η , ζ , and P_m have to be specified (but these values should not deviate by more than one order of magnitude from unity). We discuss the different possibilities for dynamos in a (ξ, Ro^{-1}) -diagram (Figure 3). Dynamo action becomes possible for dynamo numbers $C_\alpha C_\Omega \sim \text{Ro}^{-2} C_\eta^{-2} \xi^{-3} \gtrsim 10^4$: this condition is fulfilled in the shaded areas of the diagram. Furthermore, cylindrical Ω -contours can be avoided only for $\text{Ta} \sim \text{Ro}^{-2} C_\eta^{-2} \xi^{-4} P_m^{-2} \lesssim 10^4$. These two constraints leave a thin strip in the (ξ, Ro^{-1}) -diagram. However, the left-hand part cannot apply to the Sun, because the latitudinal differential rotation is too weak (cf. Paper I). To the right-hand side of the strip the ratio $C_\alpha/C_\Omega \sim \xi$ becomes too large and leads so eventually to a stationary α^2 -dynamo.

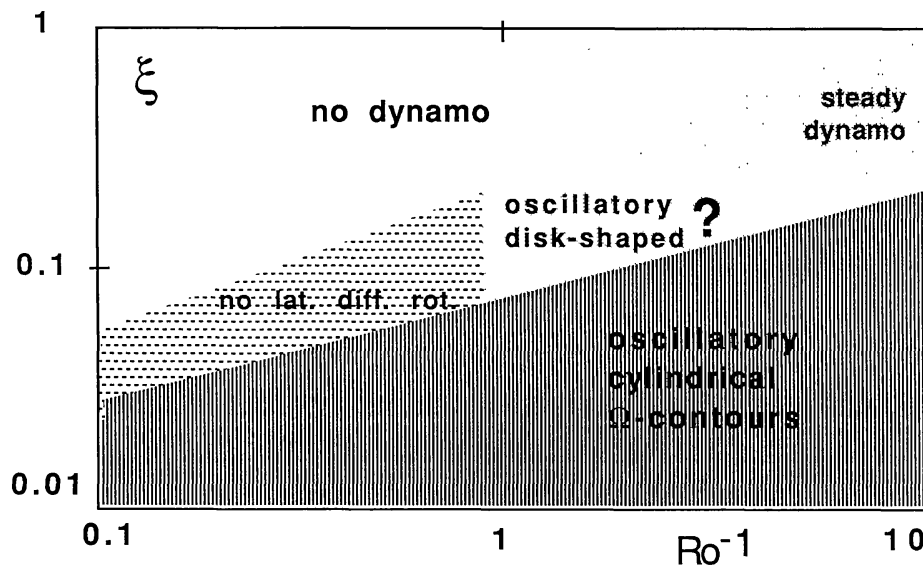


Fig. 3. A schematic state diagram for dynamos. For the Sun various constraints on an oscillatory dynamo with disk-shaped Ω -contours must determine the values for ξ and Ro^{-1} . The question mark after 'oscillatory disk-shaped' on the figure refers to the conjectural nature of such a dynamo state.

In the framework of incompressible mean-field models it has not been possible so far to solve this Taylor number puzzle of oscillatory dynamos. We expect that including more physics, such as stratification and thermodynamics, will alter some of the results substantially. For example, at the bottom of the convection zone ν_i is small and the effective Taylor number (locally) large. Thus, large radial Ω -gradients may occur which can cause an oscillatory dynamo. However, one may hope that the (ξ, Ro^{-1}) -diagram remains qualitatively correct in the sense that the solar dynamo, due to stratification, operates in different (ξ, Ro^{-1}) -states simultaneously.

References

- Brandenburg, A. and Tuominen, I.: 1988, *Adv. Space Sci.* **8**(7), 185.
- Brandenburg, A., Krause, F., and Tuominen, I.: 1989, in M. Meneguzzi, A. Pouquet, and P. L. Sulem (eds.), *Turbulence and Nonlinear Dynamics in MHD Flows*, Elsevier Science Publ. B.V. (North-Holland), Amsterdam, p. 35.
- Brandenburg, A., Krause, F., Meinel, R., Moss, D., Tuominen, I.: 1989, *Astron. Astrophys.* **213**, 411.
- Brandenburg, A., Moss, D., Rüdiger, G., and Tuominen, I.: 1990, *Astron. Astrophys.* (Paper I), (submitted).
- Brown, T. M. and Morrow, C. A.: 1987, *Astrophys. J.* **314**, L21.
- Dziembowski, W. A., Goode, P. R., and Libbrecht, K. G.: 1989, *Astrophys. J.* **337**, L53.
- Gilman, P. A. and Miller, J.: 1981, *Astrophys. J. Suppl.* **46**, 211.
- Gilman, P. A., Morrow, C. A., and DeLuca, E. E.: 1989, *Astrophys. J.* **338**, 528.
- Glatzmaier, G. A.: 1985, *Astrophys. J.* **291**, 300.
- Kichatinov, L. L.: 1987, *Geophys. Astrophys. Fluid Dyn.* **38**, 273.
- Kichatinov, L. L.: 1988, *Astron. Nachr.* **309**, 197.
- Kleorin, N. I. and Ruzmaikin, A. A.: 1982, *Magnitnaya gidrodinamika* **2**, 17.
- Krause, F. and Rädler, K.-H.: 1980, *Mean-Field Magnetohydrodynamics and Dynamo Theory*, Akademie-Verlag, Berlin.
- Libbrecht, K. G.: 1988, in E. J. Rolfe (ed.), *Seismology of the Sun and Sun-like Stars*, ESA SP-286, p. 131.
- Nordlund, Å.: 1985, *Solar Phys.* **100**, 209.
- Parker, E. N.: 1979, *Cosmical Magnetic Fields*, Clarendon Press, Oxford.
- Roberts, P. H. and Soward, A. M.: 1975, *Astron. Nachr.* **296**, 49.
- Rüdiger, G.: 1974, *Astron. Nachr.* **295**, 275.
- Rüdiger, G.: 1980, *Geophys. Astrophys. Fluid Dyn.* **16**, 239.
- Rüdiger, G.: 1989, *Differential rotation and Stellar Convection: Sun and Solar-Type Stars*, Gordon and Breach, New York.
- Rüdiger, G. and Kichatinov, L. L.: 1990, *Astron. Astrophys.* (in press).
- Tuominen, I. and Rüdiger, G.: 1989, *Astron. Astrophys.* **217**, 217.